GEOPHYSICAL RESEARCH LETTERS, VOL. 24, NO.11, PAGES 1295-1298, JUNE 1, 1997

The complex rupture process of the 1996 deep Flores, Indonesia earthquake (M_w 7.9) from teleseismic P-waves

Saskia Goes[1], Larry Ruff and Nathan Winslow

Department of Geological Sciences, University of Michigan, Ann Arbor

Abstract. From an analysis of broadband teleseismic P-waveforms we resolve the complex rupture characteristics of the 17 June 1996, Flores earthquake (M_w 7.9, depth 590 km). This earthquake was unusual because of its large rupture length and the variation in rupture velocity and stress drop. The 20 s rupture propagated westward at 2-3 km/s to a distance of 20-30 km, and eastward at 4 km/s over 75 km. Average static stress drop was about 15 MPa, but the stress drop during the episode of main moment release was a factor of four higher. The oblique normal faulting mechanism is consistent with the stress expected as the slab descends along a highly curved trench. Significant rupture complexity is also reported for the deep 1994 M_w 7.7 Fiji and M_w 8.2 Bolivia earthquakes and is evident in the source-time functions of many smaller earthquakes at depths > 300 km. Thus source complexity of deep earthquakes appears no less common than for shallow earthquakes, and requires the existence of significant heterogeneity in the physical properties that control deep earthquake rupture.

Introduction

The June 17, 1996 Flores, Indonesia, event (M_w 7.9, depth 590 km) is one of the largest deep earthquakes of the past few decades. Although it occurred at large depth, this earthquake and one of its aftershocks caused damage on the islands of Flores and Timor respectively (NEIC). The occurrence of earthquakes deeper than 300 km has puzzled scientists for many years, as brittle failure is inhibited by the high pressure at these depths. High pressure and temperature experiments have led to the proposal of several generating mechanisms. These include transformational faulting [*Kirby*, 1987; *Green and Burnley*, 1989], faulting triggered by dehydration or amorphization reactions [*Meade and Jeanloz*, 1991], reactivation of old structures in the slab [*Silver et al.*, 1995], and plastic instabilities (e.g., *Hobbs and Ord* [1988]). It remains up to seismologists to provide constraints for the alternative models.

Large deep earthquakes are rare. Since 1950 only nine earthquakes larger than M_w 7.5 at depths > 300 km have been documented (*Abe* [1982] and the Harvard CMT catalog). However, three such events occurred in 1994 and 1996. The high quality data from global broadband seismic networks available for these recent events allow us to significantly improve our knowledge of deep earthquake rupture processes. In this study we analyze broadband teleseismic P-wave records of 22 GDSN (Global Digital Seismic Network) stations to constrain the temporal and spatial distribution of moment release and the faulting mechanism of the 1996 Flores earthquake (see Figure 1 for location). The Flores rupture parameters are compared to those of the March 9, 1994 Fiji Island (M_w 7.7, depth 550 km) and the June 9, 1994, Bolivia (M_w 8.2, depth 650 km) earthquakes (e.g., *Wiens et al.* [1994], *Silver et al.* [1995], *Goes and Ritsema* [1995], *McGuire et al.* [1995]) to provide constraints on the similarities and differences between deep and shallow (< 100 km) earthquake rupture.

Directivity

P-wave displacements of deep earthquakes represent source processes only affected by attenuation and geometrical spreading. The waveforms in Figure 2 illustrate the complexity of the Flores rupture and clearly show directivity. At stations located to the north-east and east of the hypocenter (e.g. YSS and HNR in Figure 2) at least 4 subevents can be identified. At stations on the western half of the focal sphere (e.g. NWAO, CHTO and TATO) several of the initial pulses have merged. This group of subevents is marked 'A'. The last peak, marked 'B', arrives relatively late at the western stations. A change in polarity is observed at near-nodal station AAE.

The largest directivity effect is shown by the ending of the rupture marked by the arrows in Figure 2. The abrupt termination corresponds to a clear and sharp phase in the velocity recordings. The azimuthal variation of the time of this stopping phase yields a well-constrained location of the ending of subevent 'B' at 75 km from the hypocenter in a direction slightly south of east (Figure 3). Essentially the same location of the

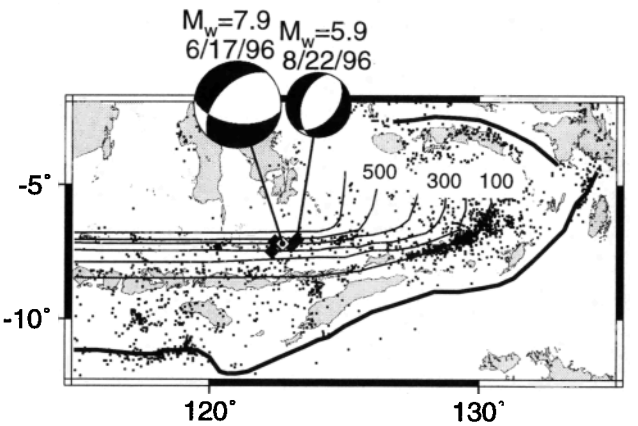

Figure 1. Seismicity (M≥5 from the PDE catalog between 1960 and 1990) around the 1996 deep Flores earthquake. Contours of seismicity drawn at 100 km depth intervals are from *Cardwell and Isacks* [1978]. Trench locations are indicated by heavy lines. Also shown are the NEIC locations of 5 aftershocks $m_b \geq 4.5$ (black diamonds). Focal mechanisms of the Flores earthquake and 1 aftershock are from the Harvard CMT catalog.

[1]presently at Geodynamics Research Instutitute, Department of Earth Sciences, Utrecht University, the Netherlands

Paper number 97GL01245.
0094-8534/97/97GL-01245$05.00

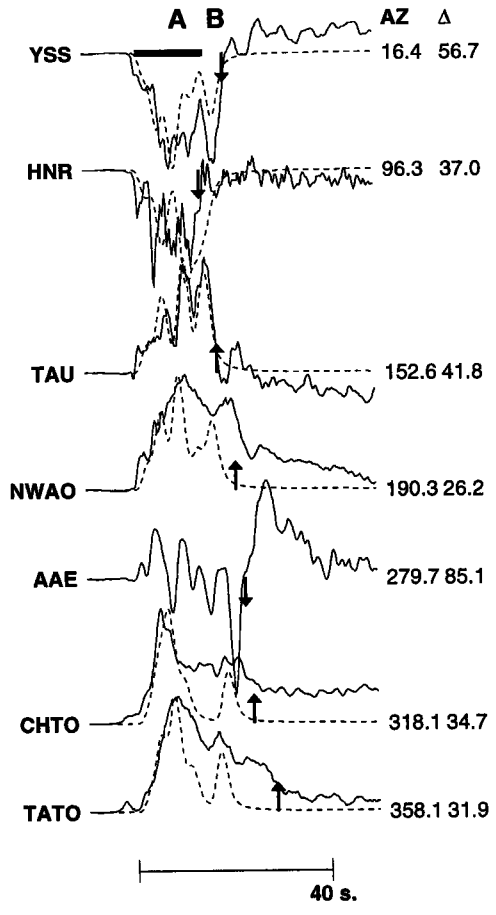

Figure 2. Representative P-wave displacement records (solid lines). Arrows mark the termination of rupture. Station codes, azimuth from north and epicentral distance in degrees are given. Synthetic seismograms for the best fitting rupture model (Figure 4) are shown with dashed lines (near-nodal station AAE was not included in this analysis).

ending is found if the nodal stations are omitted from the analysis.

In order to constrain the details of the temporal and spatial distribution of moment release we use the iterative inversion method developed by *Kikuchi and Kanamori* [1991]. Inversions are performed for various grid spacings, pulse widths and rupture geometries i.e., point, line and plane sources constrained to lie on one of the nodal planes of the P-wave mechanism obtained for 'A' (discussed below). The best waveform fit for a plane source is only slightly better (misfit of 28%) than for a point source (misfit of 34-39%). This indicates that the main area of moment release is compact. The best plane source model is presented in Figure 4. Synthetic P-wave displacements for this solution are shown in Figure 2. This model shows bi-lateral rupture on the southward dipping nodal plane (strike 112°), with a total duration of 20 s and four distinct pulses. Pulses 'A1' to 'A3' are located 10-40 km west of the hypocenter. A small subevent 'B' is located east of the hypocenter. No significant rupture along dip is resolved. Total body wave moment is in agreement with the $2.4 \cdot 10^{20}$ Nm of *Tanioka and Ruff* [Source time functions, submitted to *Seismol.. Res. Lett.*, 1996], which is 30-40% of the Harvard CMT moment estimated from long-period waves. The set of inversions indicates that the direction and rupture extent of pulses 'A1' and 'A2' are well resolved while the position of later pulses is more

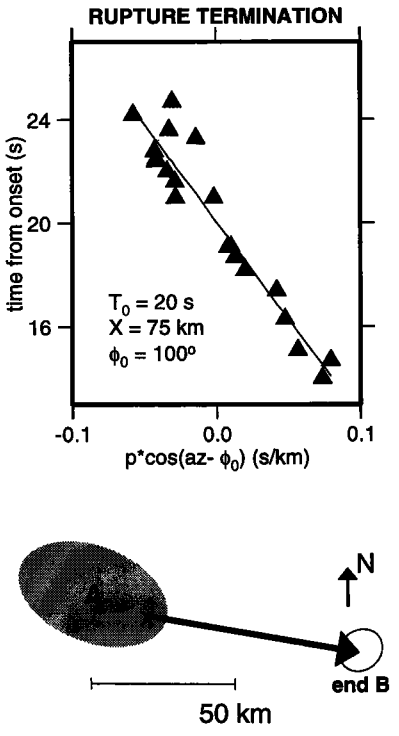

Figure 3. The location of the termination of rupture is determined by a least squares fit of the end times (Figure 2) versus the directivity parameter (equal to the ray parameter, p, times the cosine of the station azimuth, az, minus the direction of rupture, ϕ_0) (for details of this procedure see e.g., *Goes and Ritsema* [1995]; *Silver et al.* [1995]). T_0 and X are the time and distance of the rupture termination relative to the onset. The resulting location of the rupture end and standard error ellipse are shown in map view at the bottom. The area of moment release during 'A' (Figure 4) is shaded.

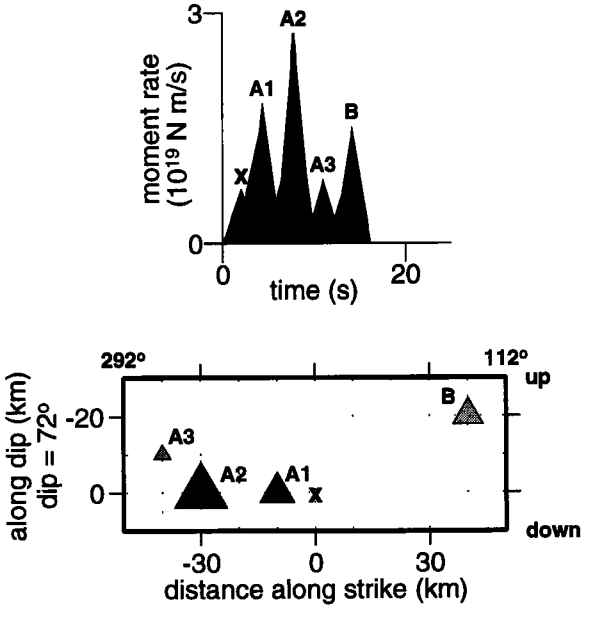

Figure 4. Representative solution of the temporal and spatial distribution of moment release determined using the inversion technique from *Kikuchi and Kanamori* [1991] with fixed mechanism ('A' in Figure 5). The main pulses of moment release are labeled 'A1' through 'A3' and 'B'. Poorly located subevents are shown as shaded rather than solid symbols. P-wave synthetics for this model are shown in Figure 2.

uncertain because the method is mainly sensitive to the strongest pulses that get stripped from the waveforms first.

Thus we resolve two distinct phases of moment release. 'A' constitutes about 75% of the moment and shows considerable complexity and a small westward directivity of 20-30 km. Final subevent 'B' ends 75 km east of the hypocenter. The 100 km long bi-lateral rupture of the Flores event is consistent with the finite fault model by *Antolik et al.* [1996], and the distribution of aftershocks [*Tinker and Wallace*, 1996; *Wiens et al.*, 1996].

Focal mechanism

Inversion of the P-waveforms for focal mechanism using the Moment Tensor Rate Function method from *Ruff and Miller* [1994] or *Kikuchi and Kanamori*'s [e.g., 1991] method yields a mechanism (Figure 5 'A') with a large strike slip component. This mechanism is representative for the main moment release 'A'. However, the displacement waveforms (Figure 2) show changes in relative amplitude between A and B at non-nodal stations and changes in polarity at nodal stations (e.g., AAE), indicative of a change in focal mechanism during rupture. This change is quantified by fitting the pattern of peak amplitudes and polarities of 'B' picked on the displacement waveforms following the procedure used by *Goes and Ritsema* [1995]. The best fit mechanism for 'B', obtained from a grid search over strike, dip and rake, is shown in Figure 5 ('B'). Thus the waveform characteristics can be modeled with a change in faulting mechanism from predominantly left-lateral strike slip for part 'A' to an oblique normal faulting mechanism similar to the Harvard CMT solution for pulse 'B'. Although this change in mechanism is small, it is resolvable from the complexity and variability it causes in the body waves.

Discussion and Conclusions

Most deep earthquakes have normal faulting mechanisms consistent with compression in down dip direction of the slab (e.g., *Frohlich* [1989]). The CMT mechanisms from earthquakes around the Flores hypocenter show a change from mainly east-west oriented normal faulting, similar to the mainshock (Figure 1), to mainly north-south oriented normal faulting for events further east, such as the easternmost aftershock in Figure 1. From the distribution of seismicity *Cardwell and Isacks* [1978] propose that the Banda slab deforms without tearing as it descends along the 90° curve in the trench (Figure 1). The CMT mechanisms of past events as well as the significant left-lateral strike-slip component in the mainshock mechanism are consistent with a counter-clockwise rotation of the slab material as it bends from an east-west to a north-south orientation. Thus the Flores mainshock may demarcate the location of the bend at 600 km depth. The change in focal mechanism during the mainshock is probably the result of additional complexity in the stresses at the bend. Other large deep earthquakes have also occurred in areas of significant subduction zone complexity. The 1994 Fiji earthquake occurred near the northern termination of the Tonga subduction zone where the seismicity indicates that the slab is highly deformed, and the 1994 Bolivia event occurred at a major bend in the Nazca slab.

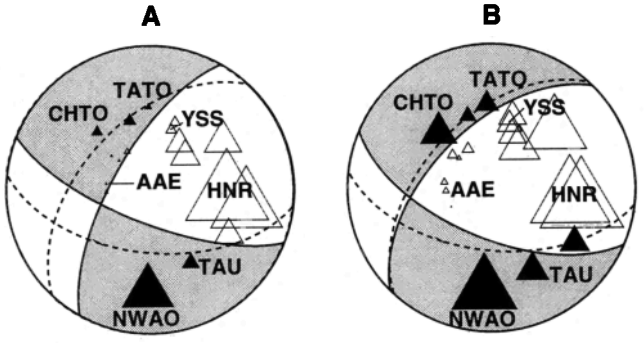

Figure 5. Best fitting focal mechanisms (shaded) and amplitudes of first (representative of group 'A') and last ('B') subevents. Open and solid triangles represent amplitudes with negative and positive polarity respectively. The triangles are scaled according to the peak amplitudes, corrected for geometrical spreading. The Harvard CMT mechanism is shown by dashed lines.

Table 1. Rupture parameters

	FIJI*	FLORES	BOLIVIA*	
Harvard CMT moment (M_0)	$2.8 \cdot 10^{20}$	$7.9 \cdot 10^{20}$	$3.0 \cdot 10^{21}$	Nm
duration	12	20	40	s
total rupture area (L·w)	40x30	105x20	65x30	km^2
area of main moment release	40x30	30x20	40x30	km^2
(% of total moment)	(100%)	(75%)	(95%)	
rupture velocity	3-4.5	2-4	1-3	km/s
stress drop ($8/3\pi \cdot M_0/w^2L$)	$7^{1,2}$	$16^1, 56^2$	71^2	MPa
average slip (M_0/mwL)	$2^{1,2}$	7.5^1	20^2	m
seismic efficiency**	0.25	0.05	0.02	

* *Goes and Ritsema* [1995]
** *Winslow and Ruff* [submitted to Geophys. J. Int. 1996]
[1] averaged over total rupture area
[2] for area of main moment release

Because the average duration for deep earthquakes is shorter (by about a factor of 2) than for shallow events of similar size (e.g., *Frohlich* [1989], *Green and Houston* [1995]) deep earthquakes are often thought to be more spatially compact. This assumes that rupture velocity (typically 2-3 km/s for shallow earthquakes) increases only slightly with depth, proportionally to the shear wave velocity. However, for the Fiji, Bolivia and Flores events a large range of rupture velocities and a similarly large variation in rupture areas is found (Table 1; *Silver et al.* [1995]; *McGuire et al.* [1995]; *Goes and Ritsema* [1995]). The Flores rupture length is similar to what is generally found for shallow earthquakes of the same size (~ 90 km), and large compared to the Fiji and Bolivia events. Static stress drop for the events ranges from values similar to those documented for shallow earthquakes (1-10 MPa) for the Fiji and the eastern part of the Flores rupture, to values an order of magnitude higher for the Bolivia event and the first 10 s of the Flores earthquake (Table 1). Seismic efficiency, the ratio of seismic wave energy over minimum static strain energy (= apparent stress / static stress drop) (e.g., *Kanamori and Anderson* [1975]) also varies considerably for the three events (1-25% Table 1). Thus simple scaling relations that assume a constant rupture velocity and/or static stress drop may not be applicable to deep earthquakes. Furthermore, the fact that deep earthquakes have higher static stress drops and a lower seismic efficiency (apparent stress stays relatively constant with depth e.g., *Green and Houston* [1995], N.W. Winslow and L.R. Ruff, Radiated energy and apparent stress drops of deep earthquakes, submitted to *Geophys. J. Int.* 1996) than shallow events may be an expression of the different failure mechanisms underlying the rupture of deep and shallow earthquakes.

In their short duration the Fiji, Bolivia and Flores events all show considerable rupture complexity. To investigate whether

this complexity is characteristic for deep events, we analyze the source-time functions (STFs) of all deep (depth ≥ 300 km) and shallow (depth 0-70 km) earthquakes with moments larger than $2.4 \cdot 10^{19}$ Nm ($M_w \geq 6.9$) in the Michigan source-time function catalog [Y.Tanioka and L. Ruff, Source time functions, submitted to *Seismol.. Res. Lett.*, 1996]. We independently classified each of the STFs as either simple or complex, using to the (qualitative) criterion that an earthquake is only simple when it consists of one pulse, i.e. a monotonic increase of moment rate followed by a monotonic decrease, with deviations from this trend less than ~10%. Only 2 out of the 9 (about 20%) deep events were classified as simple, versus 11 out of 33 (30%) shallow earthquakes. Thus there is no indication that the rupture of deep earthquakes is "simpler" than the rupture of shallow events in the same size range.

Variations in fault geometry and lithology are probable factors controlling rupture complexity in shallow earthquakes. For deep earthquakes two types of heterogeneity in the subducting slabs may play a role: (1) pre-existing strength variations due to e.g., old brittle faulting structures [*Silver et al.*, 1995], or local variations in mineralogy or water content; or (2) variations in material strength due to recent (deep) rupture. If transformational faulting causes deep earthquakes we speculate this may work as follows. The triggering of unstable slip by the phase change from metastable olivine to spinel has been proposed as a mechanism to generate new shear zones (e.g., *Green and Houston* [1995]). However, if grain growth of the superplastic spinel that forms the shear zones is slow enough (due to the low temperatures in the core of the slab), these zones of weakness may slip again in future ruptures. This is only possible if rupture, once nucleated, can propagate outside the metastable zone. There are indications that this may indeed occur [*Green and Houston*, 1995, pg. 194]. The existence of zones of weakness due to previous earthquakes may explain the correlation of high background seismicity with low static stress drop ($\Delta\sigma_s$) and high rupture velocity (V_{rup}) for the Fiji earthquake and the eastern region of the Flores rupture, and the high $\Delta\sigma_s$, and low V_{rup} for the Bolivia earthquake which occurred in an area previously devoid of seismicity. Note also that there is little seismic activity west of the Flores earthquake in which direction $\Delta\sigma_s$ was high and V_{rup} low (Figure 1; *Tinker and Wallace*, 1996; *Wiens et al.*, 1996). Furthermore, the presence of lineations in deep seismicity, found in several slabs by *Lundgren and Giardini* [1992], indicates that deep earthquakes rerupture along the same planar structures. The correlation between background seismicity and aftershock productivity with slab temperature found by *Wiens and Gilbert* [1996] may be explained by the fact that the rate of grain growth in the superplastic shear zones is highly sensitive to temperature . Whatever the deep earthquake failure mechanism may be, it will have to explain how heterogeneity in physical properties results in the complexity documented for deep earthquakes.

Acknowledgments. We thank Yuichiro Tanioka for help with running several of the programs used, Jeroen Ritsema for his comments on the manuscript, Paul Lundgren, Cliff Frohlich and an anonymous reviewer for their constructive reviews. IRIS provided the high quality seismic data analyzed in this study. This research was partially supported by NSF grant EAR-9405533 and the Geodynamics Research Institute, University of Utrecht.

References

Abe, K, Magnitude, seismic moment, and apparent stress for major deep earthquakes, *J. Phys. Earth, 30*, 321-330, 1982.

Antolik, M., D. Dreger and B. Romanowicz, Finite fault models of recent large deep earthquakes, *EOS Transactions AGU, 77*, F491, 1996. (abstract)

Cardwell, R.K., and B. L. Isacks, Geometry of the subducted lithosphere beneath the Banda Sea in eastern Indonesia from seismicity and fault plane solutions, *J. Geophys. Res., 83*, 2825-2838 1978.

Frohlich, C., The nature of deep-focus earthquakes, *Ann. Rev. Earth Planet. Sci., 17*, 227-254, 1989.

Goes, S. and J. Ritsema, A broadband P-wave analysis of the large deep Fiji Island and Bolivia earthquakes of 1994, *Geophys. Res. Lett., 22*, 2249-2252, 1995.

Green II, H.W., and H. Houston, The mechanics of deep earthquakes, *Annu. Rev. Earth Planet. Sci., 23*, 169-213, 1995.

Green II, H.W., and P.C. Burnley, A new self-organizing mechanism for deep-focus earthquakes, *Nature, 341*, 733-737, 1989.

Hobbs, B.E. and A. Ord, Plastic instabilities: implications for the origin of intermediate and deep focus earthquakes, *J. Geophys. Res., 93*, 10,521-10,540, 1988.

Kanamori, H., and D.L. Anderson, Theoretical basis of some empirical relations in seismology, *Bull. Seismol. Soc. Am., 65*, 1073-1095, 1975.

Kikuchi, M. and H. Kanamori , Inversion of complex body waves 3., *Bull. Seismol. Soc. Am., 81*, 2335-2350, 1991.

Kirby, S.H., Localized polymorphic phase transformations in high-pressure faults and applications to the physical mechanism of deep earthquakes, *J. Geophys. Res., 92*, 13,789-13,800, 1987.

Lundgren, P. and D. Giardini, Seismicity, shear failure and modes of deformation in deep subduction zones, *Phys. Earth Planet. Int., 74*, 63-74, 1992.

McGuire, J.J, D.A. Wiens, P.J. Shore, M.G. Bevis, The March 9, 1994 (Mw 7.6) deep Tonga earthquake: rupture outside the seismically active slab, *J. Geophys. Res.*, submitted, 1995.

Meade, C. and R. Jeanloz, Deep-focus earthquakes and recycling of water into the Earth's mantle, *Science, 252*, 68-72, 1991.

Ruff, L.J. and A.D. Miller, Rupture process of large earthquakes in the northern Mexican subduction zone, *Pure Appl. Geophys., 142*, 101-172, 1994.

Silver, P.G., S.L. Beck, T.C. Wallace, C. Meade, S.C. Myers, D.E. James, R. Kuehnel, The rupture characteristics of the great, deep Bolivian earthquake of 1994, and the physical mechanism of deep-focus earthquakes, *Science, 268*, 69-73, 1995.

Tinker, M.A. and T.C. Wallace, Aftershock locations of the deep 1996 Flores Sea earthquake: implications for Banda Sea tectonics, *EOS Transactions AGU, 77*, F491, 1996. (abstract)

Wiens, D.A., J. Hildebrand and W: Crawford, Source and aftershock studies of the 1995 Marianas and 1996 Flores Sea deep earthquakes, *EOS Transactions AGU, 77*, F491-F492, 1996. (abstract)

Wiens, D.A. and H.J. Gilbert, Effect of slab temperature on deep-earthquake aftershock productivity and magnitude-frequency relations, *Nature, 384*, 153-156, 1996.

S.D.B. Goes, Geodynamics Research Instutitute, Department of Earth Sciences, Utrecht University, P.O. Box 80.021, 3508 TA Utrecht, the Netherlands (e-mail: saskia@geof.ruu.nl)

L.J. Ruff and N. Winslow, Department of Geological Sciences, University of Michigan,, Ann Arbor, MI 49109 (ruff@umich.edu, natemail@geo.lsa.umich.edu)

(Received: September 23, 1996; Revised: January 3, 1997;
Accepted: April 15, 1997.)